

---

---

PRODUCTION, STRUCTURE, PROPERTIES

---

---

# Phase Formation and Physical and Mechanical Properties of Fe–Cu–Ni–Sn–VN Composites Sintered by Vacuum Hot Pressing for the Diamond Stone Processing Tools

V. A. Mechnik<sup>a, \*</sup>, N. A. Bondarenko<sup>a</sup>, T. A. Prikhna<sup>a</sup>, V. M. Kolodnitskyi<sup>a, \*\*</sup>, V. E. Moshchil<sup>a</sup>,  
V. V. Strelchuk<sup>b</sup>, A. S. Nikolenko<sup>b</sup>, E. S. Gevorkyan<sup>c</sup>, and V. A. Chishkala<sup>d</sup>

<sup>a</sup> *Bakul Institute for Superhard Materials, National Academy of Sciences of Ukraine, Kyiv, Ukraine*

<sup>b</sup> *Lashkaryov Institute of Semiconductor Physics, National Academy of Sciences of Ukraine, Kyiv, Ukraine*

<sup>c</sup> *Ukrainian State University of Railway Transport, Kharkiv, Ukraine*

<sup>d</sup> *Karazin Kharkiv National University, Kharkiv, Ukraine*

\**e-mail: vlad.me4nik@ukr.net*

\*\**e-mail: vasykolod56@gmail.com*

Received July 5, 2021; revised July 29, 2021; accepted August 9, 2021

**Abstract**—The effect of the concentration of vanadium nitride additive (in the range from 0 to 10 wt %) on the phase formation, hardness, and fracture toughness of composite diamond-containing materials based on the 51Fe–32Cu–9Ni–8Sn matrix molded by cold pressing and subsequent vacuum hot pressing is investigated. It is found that the addition of 10 wt % of vanadium nitride to the 51Fe–32Cu–9Ni–8Sn composite is accompanied by an increase in the hardness from 3.86 to 8.58 GPa with a slight decrease in the fracture toughness from 5.55 to 4.76 MPa m<sup>1/2</sup>. Moreover, the  $H(C_{VN})$  dependence has two characteristic segments that differ in the slope. The hardness increases insignificantly (from 3.86 to 5.26 GPa) in the range of  $0 < C_{VN} < 4$  wt %, while the second region ( $C_{VN} > 4$  wt %) is characterized by a more substantial increase in the hardness and a more significant decrease in the grain size. It is shown that these parameters are achieved owing to the dispersion mechanism of strengthening and modification of the structure (a decrease in the mean particle size of the matrix phase, the formation of new (Fe<sub>3</sub>Ni)<sub>0.5</sub> and Cu<sub>3</sub>Fe<sub>17</sub> phases, and the precipitation of primary and secondary phases of vanadium nitride) and phase composition of the composites.

**Keywords:** composite, iron, copper, nickel, tin, vanadium nitride, composition, concentration, vacuum hot pressing, structure, hardness, fracture toughness

**DOI:** 10.3103/S1063457622030066

## INTRODUCTION

The creation of composite diamond-containing materials (CDMs) based on metal matrices containing iron, copper, nickel, and tin (C<sub>diamond</sub>–Fe–Cu–Ni–Sn) is of special interest for structural and functional applications [1–5]. This is because such CDMs are widely used for the manufacture of cutting wheels, rope saws, drill bits, and grinding and polishing tools for the stone and mining industries [6–10]. The undoubted advantage of such CDMs in comparison with CDMs based on cobalt matrices is their plasticity and good cutting properties, as well as low cost of iron and its nontoxicity. The interest in such materials is also driven by the possibility of achieving high strength characteristics and maintaining a high level of cutting properties at the same time [11, 12]. However, it is known that the action of high contact loads [13] and temperatures [14–16] during operation results in deteriorating the elastic properties of the matrix [17, 18], which leads to a decrease in the wear resistance of a CDM [19–21]. Therefore, studies on increasing the wear resistance of existing CDMs and creating new CDMs with the necessary set of physical and mechanical properties are especially relevant [22–24].

The vacuum hot pressing is a promising method that can improve the properties of diamond composites. In the case of using this method, the recrystallization during sintering is prevented either by lowering the temperature and reducing the duration of sintering [25, 26] or by optimizing the shrinkage processes [27]. To increase the quality level of mechanical properties of CDMs under consideration, additives of transition metal compounds are introduced into their composition in quantities that are small compared

to those of the main components [30, 31]. As was shown in [32, 33], the addition of up to 2 wt % of  $\text{CrB}_2$  to the composition of the matrix of the 51Fe–32Cu–9Ni–8Sn<sup>1</sup> composite sintered at 800°C with subsequent hot pressing increases its wear resistance as a result of the binding of carbon that appears during graphitization of diamond grains into nanoscale thick carbides  $\text{Fe}_3\text{C}$ ,  $\text{Cr}_3\text{C}_2$ ,  $\text{Cr}_7\text{C}_3$ , and  $\text{Cr}_{1.65}\text{Fe}_{0.35}\text{B}_{0.95}$ . As was found in [34], the hardness and elastic modulus of the 51Fe–32Cu–9Ni–8Sn composite sintered at 800°C with subsequent hot pressing increases with an increase in the concentration of  $\text{CrB}_2$  (in the range from 0 to 8 wt %). At the same time, the coefficient of friction and the wear rate decrease with an increase in the concentration of  $\text{CrB}_2$  to 2% and then increase with a further increase in the concentration of  $\text{CrB}_2$  [35].

As was revealed in [36], the addition of  $\text{CeO}_2$ ,  $\text{LaO}_3$ ,  $\text{Y}_2\text{O}_3$ , and  $\text{V}_2\text{O}_5$  to the CDM composition based on a Fe-containing matrix sintered by hot pressing at a temperature of 700°C helps to improve the retainability of diamonds and to increase the wear resistance of the composite. As was shown in [37], the problem of strengthening and improving the mechanical properties of hot-pressed CDMs based on the Fe–Cu–Ni–Sn matrices at 900°C and 25 MPa can be solved by introducing the  $\text{Al}_2\text{O}_3$  and  $\text{Al}_{14}\text{C}_3$  micropowder additives. In [38], the effect of the addition of  $\text{SiC}$ ,  $\text{Al}_2\text{O}_3$ , and  $\text{ZnO}_2$  micropowders on the hardness and wear resistance of CDMs based on the Fe–Mn–Cu–Sn matrices and prepared by spark plasma sintering (SPS) was studied. Prospects for the use of these CDMs for the development of high performance diamond tools are shown. The best indexes of mechanical properties were achieved with a processing temperature of 840°C and a pressure of 25 MPa.

Vanadium nitride (VN) is promising for the use as a strengthening phase of CDM based on the Fe–Cu–Ni–Sn matrix [25]. Vanadium nitride has a lower dissolution temperature in  $\gamma$ -Fe compared to carbides, borides, silicides, and other transition metal compounds. In addition, vanadium nitride has a smaller crystal lattice parameter compared to other transition metal compounds, which provides minimal dilatation at the nitride–matrix interface [39]. These two factors contribute to achieving a greater effect of strengthening and increasing the wear resistance of the 49.47Fe–31.04Cu–8.73Ni–7.76Sn–3VN composite formed by cold pressing and subsequent vacuum hot pressing at 1000°C under a pressure of 30 MPa in comparison with the 51Fe–32Cu–9Ni–8Sn composite formed under the same conditions [40]. The mechanism of improving the properties of the 49.47Fe–31.04Cu–8.73Ni–7.76Sn–3VN composite is that VN dissolves in  $\gamma$ -Fe during sintering and precipitates as a fine-grained phase during cooling [26, 41, 42]. As was also noted in [43–45], grain size reduction in composites of other systems in the process of sintering helps to increase their mechanical and operational properties.

At the same time, there are practically no published data on the formation of phases and on the mechanical and operational properties of the considered composites with different contents of VN additive. Numerous experimental data confirm that the samples of such composites, which differ in composition and technological regimes of the manufacture, show a substantial variation in physical and mechanical properties. A change in the additive concentration often leads to changes in important characteristics of composite materials, such as the hardness, modulus of elasticity, fracture toughness, ductility, friction coefficient of, wear resistance, etc. The properties (ratio of characteristics) of the composite (Fe–Ni–Cu–Sn–VN) can be arbitrarily controlled due to the variability of its composition and structure. Variation of these factors allows one to control the ratio of hardness, fracture toughness, and wear resistance.

The aim of this study was to investigate the effects of the addition of a dispersive VN powder in concentrations from 0 to 10% to diamond-containing materials, which are formed by cold pressing and subsequent vacuum hot pressing and used in stone-cutting tools for various technological purposes, on the formation of phases, the hardness, and the crack resistance of the matrix material based on the 51Fe–32Cu–9Ni–8Sn composite.

## EXPERIMENTAL

### *Starting Materials and Sintering Methods*

Iron powder PZh1M2, copper powder PMS-1, nickel powder PNE, tin powder PO-1 (State Enterprise Powder Metallurgy Plant, Zaporizhzhia, Ukraine), and vanadium nitride (CASRN 24646-85-3, ONYX-MET, Poland) were used for sintering of composite samples. The mean particle sizes were as follows:  $d \approx 25 \pm 10 \mu\text{m}$  for the iron powder,  $d \approx 20 \pm 9 \mu\text{m}$  for the copper powder,  $d \approx 15 \pm 8 \mu\text{m}$  for the nickel powder,  $d \approx 15 \pm 8 \mu\text{m}$  for the tin powder, and  $d \approx 0.5 \pm 0.1 \mu\text{m}$  for VN. The compositions of the initial mixtures and samples of composites are given in Table 1.

<sup>1</sup> Hereafter, the compositions of CDMs are given in wt %.

**Table 1.** Composition of the initial mixtures and sintered samples of composites (wt %)

Sample	Fe	Cu	Ni	Sn	VN
1	51	32	9	8	–
2	50.745	31.84	8.955	7.96	0.5
3	50.49	31.68	8.91	7.92	1
4	50.235	31.52	8.865	7.88	1.5
5	49.98	31.36	8.82	7.84	2
6	48.96	30.72	8.64	7.68	4
7	47.94	30.08	8.46	7.52	6
8	46.92	29.44	8.28	7.36	8
9	45.9	28.8	8.1	7.2	10

The powders were dry mixed in a mixer with a shifted axis of rotation for 8 h. The specific power of the mixer was 8 W/h. The prepared mixtures were pressed using a hydraulic press in molds made of heat resistant alloys at room temperature under a pressure of 500 MPa. The briquettes were sintered in graphite molds by vacuum hot pressing in the temperature range of 20–1000°C under a pressure of 30 MPa for 5 min [46]. After sintering, the sample billets were ground to obtain cylinders with a diameter of 9.62 mm and a thickness of 4.84 mm. Before conducting microstructural and mechanical tests, the surfaces of the sintered samples were polished using a diamond paste with a particle size of 1 μm and a colloidal solution of silicon oxide particles with a size of 0.04 μm to obtain a mirror surface.

#### *X-ray Diffraction Structural Studies and Micromechanical Properties of Samples*

The crystal structure and phase composition of sintered samples of composite materials were studied by X-ray diffractometry (XRD) using a DRON-4 diffractometer with a  $\text{CuK}_\alpha$  radiation source ( $\lambda_{\text{Cu}} = 0.1542$  nm). Crystalline phases in the samples were identified using the method of X-ray diffractometry.

A Falcon 500 microhardness tester (Innovates, Holland) equipped with a five-megapixel digital microscope was used to determine Vickers hardness and visualize indenter imprints under a load of 25 N, and to measure the radial crack lengths. To calculate the microhardness and crack resistance, the Falcon 500 microhardness tester was equipped with the Impressions software package, which allowed us to determine the mechanical characteristics in a semiautomatic mode.

The microhardness was determined by the following formula:

$$H_V = 463.6 \frac{F}{d_{\text{mean}}},$$

where  $F$  is the load on the indenter in N, and  $d_{\text{mean}} = (d_1 + d_2)/4$  is the half of the average length of the imprint diagonal in μm.

Fracture toughness  $K_{Ic}$  of the composite was determined according to [47] from the following expression:

$$\frac{K_{Ic} \Phi}{Hd^{0.5}} = 0.15k \left( \frac{C}{d} \right)^{-1.5}.$$

where  $\Phi$  is the constraint factor ( $\sim 3$ ),  $H$  is the Vickers hardness,  $C = (C_1 + C_2)/2$  is the average length of radial cracks measured from the center of the imprint, and  $k = 3.2$ . The value of the  $k$  factor was determined empirically using the  $K_{Ic}$  values measured by standard methods in macroscopic samples.

Considering the relationship for the Vickers hardness and the formula introduced by Evans and Charles, the final formula for determining the crack resistance looks as follows:

$$K_{Ic} = 7.42 \times 10^{-2} \frac{F}{C^{1.5}}.$$

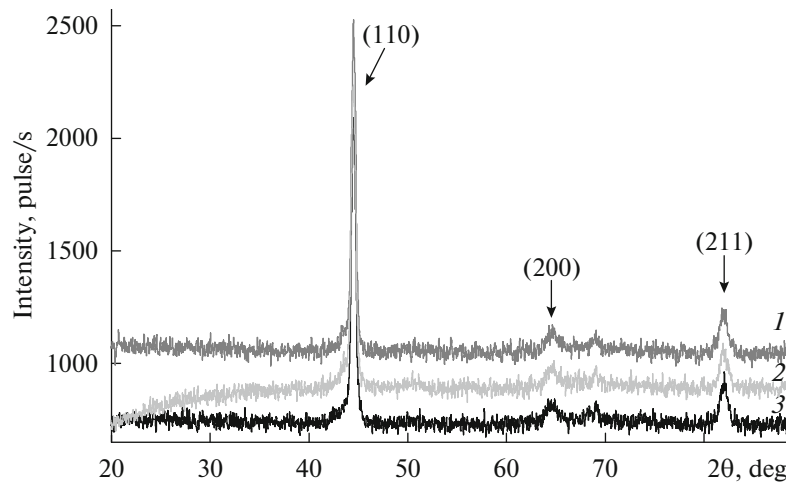


**Fig. 1.** X-ray diffraction patterns of the 51Fe–32Cu–9Ni–8Sn matrix materials with different contents of VN (samples 1–3). For better perception, the X-ray diffraction patterns in this and further figures are shifted in the vertical direction.

## RESULTS AND DISCUSSION

### *Morphology of Starting Materials*

The morphology of bulk powders of iron, copper, nickel, and tin, and the initial mixtures for sintering samples of composite materials have been studied in [48], so we just summarize these results. As was shown in [48], there are no defects (cracks and chips) on the surface of diamond grains, which is an indication of their quality. Iron powder particles with a mean size of 25  $\mu\text{m}$  have an irregular shape. Larger iron particles formed by the adhesion of smaller agglomerate particles are also observed. Copper powder particles with a size of 20  $\mu\text{m}$  have a less dense and thinner spatial dendritic structure with pronounced branches, which reduces the relative bulk density and prevents them from dense packing in bulk. Nickel powder particles with a mean size of 15  $\mu\text{m}$  have a rounded shape and a very dense structure, which leads to a high packing density in bulk like in iron powders. Tin powder particles with a mean size of 15  $\mu\text{m}$  have a rounded shape, though there are also elongated particles. Inflows of metal and small particles (satellites) were observed on their surface. The rounded shape of the particles well contributes to their dense packing in bulk. According to [25], the particles of vanadium nitride powder have a ternary structure, namely: VN (cubic) with a crystal lattice parameter of  $a = 0.4136$  nm and  $\text{VO}_2$  (hexagonal) with crystal lattice parameters of  $a = 0.5743$  nm,  $b = 0.4517$  nm, and  $c = 0.5375$  nm, which are in good agreement with the data of the ICPDS–ASTM database [49]. The particle size of the VN powder is in the range from 0.1 to 0.7  $\mu\text{m}$  (mean size  $\sim 0.5$   $\mu\text{m}$ ). Relatively uniform distribution of components was observed in the initial mixtures, which is important for the subsequent sintering of composite samples.

### *Powder X-ray Diffraction*

Figure 1 shows X-ray diffraction patterns of the 51Fe–32Cu–9Ni–8Sn matrix material formed using the cold pressing method followed by vacuum hot pressing with different contents of VN additives. As can be seen from Fig. 1, the same set of (110), (200), and (211) reflections of the cubic phase—the crystal lattice parameter of which is  $a = 0.28741$  nm—was recorded in the X-ray diffractograms of studied samples 1–3. The diffracton peak intensities of the (110), (200), and (211) reflections decrease in the lattice of samples 1 and 2. This indicates a lower coefficient of crystallinity in these samples compared to sample 3. It should be noted that the Fe,  $(\text{Fe}_3\text{Ni})_{0.5}$ ,  $\text{Cu}_3\text{Fe}_{17}$ , and some others phases have similar crystal lattice parameters. The X-ray diffraction data cannot exactly determine which phase or their superposition is present in these samples. However, the Fe,  $(\text{Fe}_3\text{Ni})_{0.5}$ , and  $\text{Cu}_3\text{Fe}_{17}$  phases may be present in their composition if we consider the chemical composition of samples 1–3.

In sample 4 (Fig. 2), there is a strong peak at 53.40 degrees and other peaks of the cubic phase of Cu with a parameter of  $a = 0.36078$  nm (75%) and the  $\text{FeNi}_3$  phase with a parameter of  $a = 0.35523$  nm (25%).

The positions of diffraction peaks in samples 5–7 are shifted (Fig. 3), which may be associated with deformations of the phases that are present in samples 1–3 and copper or the emergence of new phases with different stoichiometry and new lattice parameters.

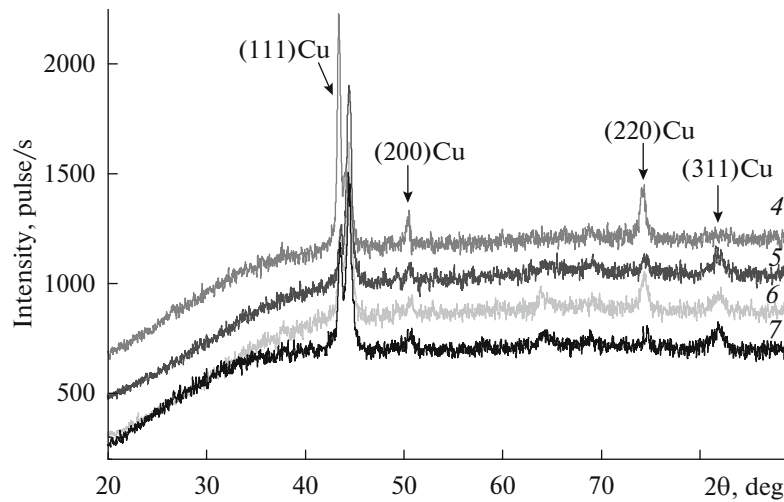


Fig. 2. X-ray diffraction patterns of the 51Fe–32Cu–9Ni–8Sn matrix materials with different contents of VN (samples 4–7).

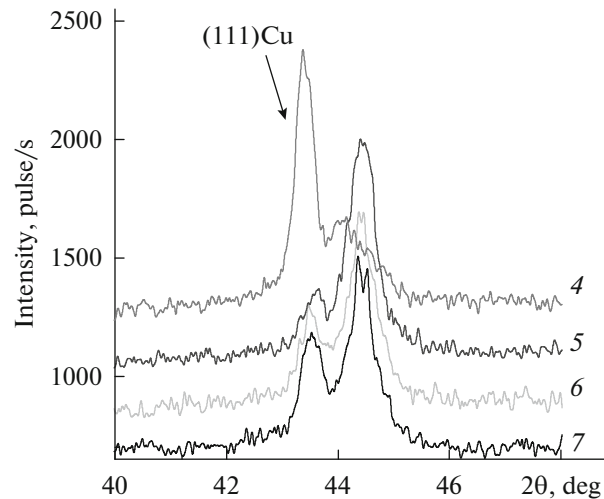


Fig. 3. X-ray diffraction patterns of the 51Fe–32Cu–9Ni–8Sn matrix materials with different contents of VN (samples 4–7) in the region of the Cu (111) reflection.

Thus, the diffraction peaks in the X-ray diffractograms of samples 8 and 9 indicate a decrease in the grain size compared to that of samples 1–7.

As a result, an increase in the parameter of crystalline lattices from  $a = 0.28741$  nm in samples 4–9 containing vanadium nitride additives in concentrations from 1.5 to 10% to  $a = 0.4124$  nm in samples 1–3 containing vanadium nitride additives in smaller amounts (from 0 to 1%) was observed, which may be caused by deformations of the phases that are present in samples 1–3 and copper or the emergence of new phases with different stoichiometry and new lattice parameters. At the same time, vanadium nitride partially dissolves in  $\gamma$ -Fe at a temperature of  $\sim 980^\circ\text{C}$  during sintering of samples 4–9 and is released as an independent dispersed phase with simultaneous grain disintegration during cooling [25]. All this can have an effect on the physical and mechanical properties of sintered composites.

#### *Mechanical Properties of Samples*

A substantial increase in the hardness measured by Vickers pyramid indentation of sintered 51Fe–32Cu–9Ni–8Sn composites was revealed with an increase in the VN concentration. The effects of the content of VN on the mean measured hardness values ( $H$ ) of sintered samples of the 51Fe–32Cu–9Ni–

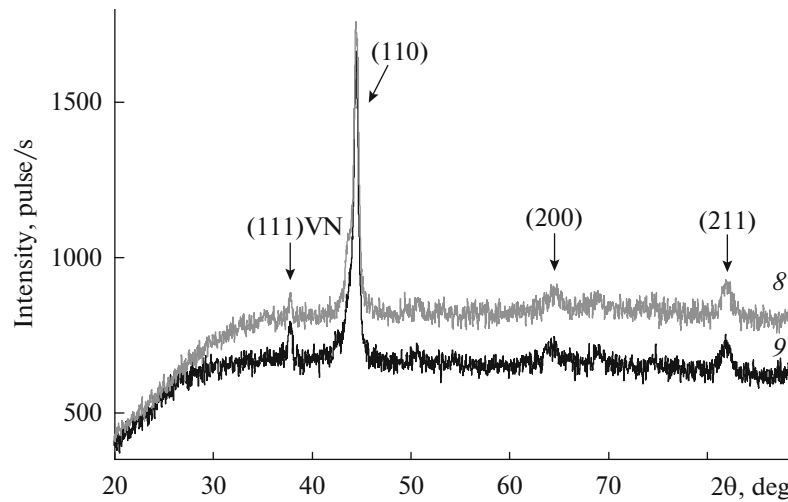


Fig. 4. X-ray diffraction patterns of the 51Fe–32Cu–9Ni–8Sn matrix materials with different contents of VN (samples 8 and 9).

8Sn composite and on the calculated critical crack resistance coefficient (fracture toughness) are shown in Fig. 5. As seen from curve 1 (Fig. 5a), the  $H(C_{\text{VN}})$  dependence has two characteristic segments that differ in the slopes. In the range of  $0 < C_{\text{VN}} < 4\%$ , the hardness increases slightly (from 3.86 to 5.26 GPa). The second region ( $C_{\text{VN}} > 4\%$ ) is characterized by a more substantial increase in the hardness. Thus, the hardness in the case of  $C_{\text{VN}} = 10\%$  increases to 8.58 GPa. As a result, it is found that the  $H(C_{\text{VN}})$  dependence has a maximum at  $C_{\text{VN}} = 10\%$ . It should be noted that VN acts as a strengthening additive in the 51Fe–32Cu–9Ni–8Sn composite and has a positive effect on its structure (causes fragmentation of the structure) [25] and mechanical properties (increases hardness and wear resistance) [41]. The effect of CrB<sub>2</sub> added in the amount of 2% and technological regimes of hot pressing on the strength characteristics of the matrix material of the 51Fe–32Cu–9Ni–8Sn CDM was studied in [33]. It was found that the addition of 2% CrB<sub>2</sub> to the composition of the 51Fe–32Cu–9Ni–8Sn composite increases its microhardness from 2.93 to 4.12 GPa. Comparison of the obtained results with the published data [33] shows the promising potential of the developed composites for the use in stone cutting tools for various technological purposes.

On the contrary, the study of vanadium nitride content in the composition of the 51Fe–32Cu–9Ni–8Sn composite revealed a slight decrease in fracture toughness  $K_{\text{Ic}}$ . The maximum value equal to  $K_{\text{Ic}} = 5.35 \text{ MPa m}^{1/2}$  was observed in sample 1 with zero concentration of vanadium nitride. At the same time, the matrix material is barely destroyed in the vicinity of the imprint (cracks are almost invisible). As was found from microindentation of sample 2 ( $C_{\text{VN}} = 0.5\%$ ), the fracture toughness decreased to  $K_{\text{Ic}} = 5.16 \text{ MPa m}^{1/2}$  and cracks slightly larger than those in sample 1 were observed in the matrix near the indenter imprint. A further increase in the content of VN in the composition of the 51Fe–32Cu–9Ni–8Sn composite leads to a further insignificant decrease in the fracture toughness. This fact is nontrivial and noteworthy, since the structural changes in the material usually affect the hardness and fracture toughness in different ways. Figures 5b–5d show, as an example, the microphotographs of Vickers pyramid imprints formed in samples of the 51Fe–32Cu–9Ni–8Sn with vanadium nitride concentrations of 0, 4, and 10% (samples 1, 6, and 9, respectively). The appearance of pronounced radial cracks in the vicinity of the Vickers pyramid imprints in samples 6 and 9 (see Figs. 5c and 5d) in comparison with sample 1 (see Fig. 5b) indicates some embrittlement of the material containing the VN additive in the amounts of 4 and 6%, respectively.

The observed nonmonotonic dependences of the strength of the studied composites on the VN content are the result of a complex combination of the dispersion mechanism of strengthening and modification of the structure and phase composition of the composites. It should be noted that the efficiency of the mechanism of dispersion hardening increases with an increase in concentration  $C_{\text{VN}}$ , but the maximum values of fracture toughness are reached at  $C_{\text{VN}} = 0$ . Such a change in the properties of sintered composites may correspond to changes in the phase composition after sintering and formation of the final structure.

Therefore, the absence of a direct dependence of the structural changes on the phase composition of the 51Fe–32Cu–9Ni–8Sn composite and the contribution of the mechanism of dispersion hardening to the concentration of VN cause nonlinear behavior of the  $H(C_{\text{VN}})$  and  $K_{\text{Ic}}(C_{\text{VN}})$  dependences.

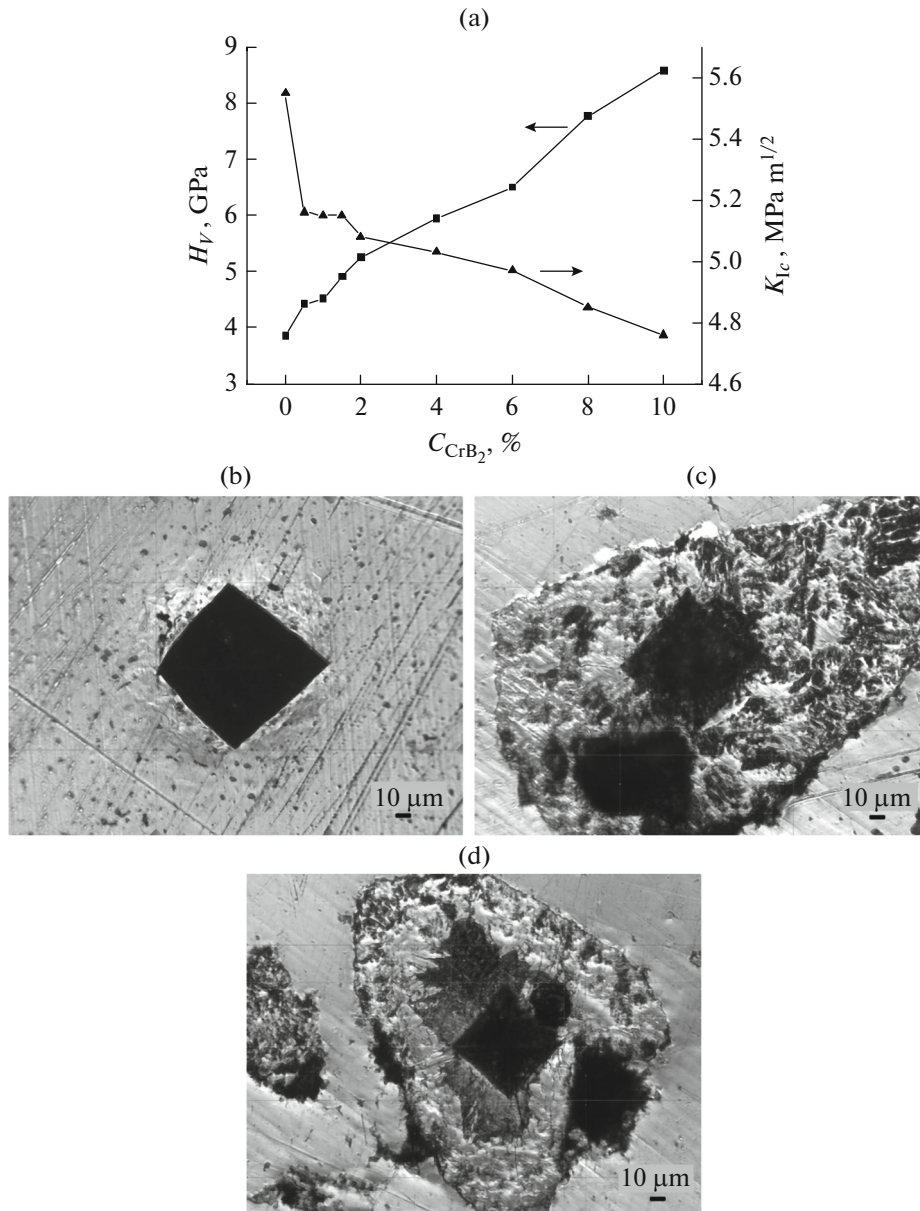


**Fig. 5.** (a) Dependences of the hardness and fracture toughness of the 51Fe–32Cu–9Ni–8Sn alloy samples on the concentration of VN, and microphotographs of the indenter imprints formed in the 51Fe–32Cu–9Ni–8Sn samples with vanadium nitride concentrations  $C_{VN}$  of (b) 0, (c) 4, and (d) 10 wt %.

Thus, it is experimentally confirmed that the use of vanadium nitride micropowder for the production of CDMs based on metal matrices with high mechanical properties by cold pressing and subsequent vacuum hot pressing is promising for the production of highly efficient tools used in the stone cutting industry. At the same time, it is necessary to strictly adhere to the optimal ratio of components, since exceeding the threshold value of the VN concentration gives rise to some decrease in the fracture toughness and may reduce the wear resistance of the composite.

## CONCLUSIONS

The addition of vanadium nitride has an effect on the phase formation and mechanical properties of samples based on the 51Fe–32Cu–9Ni–8Sn composite formed by the method of cold pressing and subsequent vacuum hot pressing. The nature of the effect and the effectiveness of the additive depend on the concentration of VN.



Sintered samples of the 51Fe–32Cu–9Ni–8Sn composites with VN contents in the range from 0 to 1% (samples 1–3) consist of the Cu, Fe, (Fe<sub>3</sub>Ni)<sub>0.5</sub>, and Cu<sub>3</sub>Fe<sub>17</sub> structural phases. An increase in crystal lattice parameter  $a$  from 0.28741 nm in samples 4–9 containing vanadium nitride additives from 1.5 to 10% to 0.4124 nm compared with samples 1–3 is observed, which may be caused by deformations of the phases that are present in samples 1–3 and Cu or the emergence of new phases with different stoichiometry and new lattice parameters. Moreover, an additional VN phase with a lattice parameter of  $a = 0.4124$  nm is present.

The addition of 10% vanadium nitride to the composition of the 51Fe–32Cu–9Ni–8Sn composite causes a substantial increase in the Vickers hardness at a load of 25 N (from 3.86 to 8.58 GPa) with a slight decrease in the fracture toughness (from 5.55 to 4.76 MPa m<sup>1/2</sup>). At the same time, the  $H(C_{VN})$  dependence has two characteristic segments that differ in the slope. The hardness slightly increases in the range of  $0\% < C_{VN} < 4\%$  (from 3.86 to 5.26 GPa), while the second segment ( $C_{VN} > 4\%$ ) is characterized by a more substantial increase in the hardness.

The nonmonotonic dependences of the strength of the studied composites on the VN content are caused by a complex combination of the dispersion mechanism of strengthening and modification of the structure and phase composition of the composites. At the same time, samples of the 51Fe–32Cu–9Ni–8Sn composites with vanadium nitride concentrations of 4, 6, 8, and 10% (samples 6–9, respectively) show an increase in crystal lattice parameter  $a$  from 0.28741 to 0.4124 nm, which may be a result of phase deformations present in samples 1–3 and the Cu phase or the emergence of new phases with different stoichiometry and new lattice parameters.

The synthesis of Fe–Cu–Ni–Sn–VN composite materials with enhanced physical and mechanical properties is important for developing tools for various technological purposes, increasing their reliability, and improving the performance.

#### FUNDING

This study was performed within the framework of State Budget Research Topics in accordance with Coordination Plans of the Ministry of Education and Science of Ukraine (State registration no. 0120U100105).

#### CONFLICT OF INTEREST

The authors declare that they have no conflicts of interest.

#### REFERENCES

1. Tillmann, W., Ferreira, M., Steffen, A., Rüster, K., Möller, J., Bieder, S., Paulus, M., and Tolan, M., Carbon reactivity of binder metals in diamond-metal composites—characterization by scanning electron microscopy and X-ray diffraction, *Diamond Relat. Mater.*, 2013, vol. 38, pp. 118–123.
2. Li, M., Sun, Y., Meng, Q., Wu, H., Gao, K., and Liu, B., Fabrication of Fe-based diamond composites by pressureless infiltration, *Materials*, 2016, vol. 9, no. 12, p. 1006.
3. Gevorkyan, E., Mechnik, V., Bondarenko, N., Vovk, R., Lytovchenko, S., Chishkala, V., and Melnik, O., Peculiarities of obtaining diamond–(Fe–Cu–Ni–Sn) composite materials by hot pressing, *Funct. Mater.*, 2017, vol. 24, no. 1, pp. 31–45.
4. Hou, M., Guo, S., Yang, L., Gao, J., Peng, J., Hu, T., Wang, L., and Ye, X., Fabrication of Fe–Cu matrix diamond composite by microwave hot pressing sintering, *Powder Technol.*, 2018, vol. 338, pp. 36–43.
5. Borowiecka-Jamrozek, J.M., Konstanty, J., and Lachowski, J., The application of a ball-milled Fe–Cu–Ni powder mixture to fabricate sintered diamond tools, *Arch. Foundry Eng.*, 2018, vol. 18, no. 1, pp. 5–8.
6. Tönshoff, H.K., Hillmann-Apmann, H., and Asche, J., Diamond tools in stone and civil engineering industry: Cutting principles, wear and applications, *Diamond Relat. Mater.*, 2002, vol. 11, nos. 3–6, pp. 736–741.
7. Dormishi, A., Ataei, M., Mikaeil, R., Khalokakaei, R., and Haghshenas, S.S., Evaluation of gang saws' performance in the carbonate rock cutting process using feasibility of intelligent approaches, *Eng. Sci. Technol. Int. J.*, 2019, vol. 22, no. 3, pp. 990–1000.
8. Borowiecka-Jamrozek, J., Konstanty, J., and Lachowski, J., The application of a ball-milled Fe–Cu–Ni powder mixture to fabricate sintered diamond tools, *Arch. Foundry Eng.*, 2018, vol. 18, pp. 5–8.
9. Konstanty, J., Romański, A., Baczek, E., and Tyrala, D., New wear resistant iron-base matrix materials for the fabrication of sintered diamond tools, *Arch. Metall. Mater.*, 2015, vol. 60, pp. 633–637.
10. Hou, M., Wang, L., Guo, S., Yang, L., Gao, J., Hu, T., and Ye, X., Fabrication of FeCu matrixed diamond tool bits using microwave hot-press sintering, *J. Sci. Eng.*, 2019, vol. 44, pp. 6277–6284.



11. Mechnyk, V.A., Diamond–Fe–Cu–Ni–Sn composite materials with predictable stable characteristics, *Mater. Sci.*, 2013, vol. 48, no. 5, pp. 591–600.
12. Mechnik, V.A., Production of diamond–(Fe–Cu–Ni–Sn) composites with high wear resistance, *Powder Metall. Met. Ceram.*, 2014, vol. 52, nos. 9–10, pp. 577–587.
13. Aleksandrov, V.A., Akeksenko, N.A., and Mechnik, V.A., Study of force and energy parameters in cutting granite with diamond disc saws, *Sov. J. Superhard Mater.*, 1984, vol. 6, no. 6, pp. 46–52.
14. Dutka, V.A., Kolodnitskij, V.M., Zabolotnyj, S.D., Sveshnikov, I.A., and Lukash, V.A., Simulation of the temperature level in rock destruction elements of drilling bits, *Sverkhtverd. Mater.*, 2004, vol. 26, no. 2, pp. 66–73.
15. Dutka, V.A., Kolodnitskij, V.M., Mel'nichuk, O.V., and Zabolotnyj, S.D., Mathematical model for thermal processes occurring in the interaction between rock destruction elements of drilling bits and rock mass, *Sverkhtverd. Mater.*, 2005, vol. 27, no. 1, pp. 67–77.
16. Sveshnikov, I.A. and Kolodnitsky, V.N., Optimization of the hard alloy cutter arrangement in the drilling bit body, *Sverkhtverd. Mater.*, 2006, vol. 28, no. 4, pp. 70–75.
17. Zhukovskij, A.N., Majstrenko, A.L., Mechnik, V.A., and Bondarenko, N.A., The stress-strain state of the bonding around the diamond grain exposed to normal and tangent loading components. Part 1. Model, *Trenie Iznos*, 2002, vol. 23, no. 2, pp. 146–153.
18. Zhukovskij, A.N., Majstrenko, A.L., Mechnik, V.A., and Bondarenko, N.A., Stress-strain state of the matrix around the diamond grain exposed to the normal and tangent loading components. Part 2. Analysis, *Trenie Iznos*, 2002, vol. 23, no. 4, pp. 393–396.
19. Aleksandrov, V.A. and Mechnik, V.A., Effect of heat conduction of diamonds and heat-exchange coefficient on contact temperature and wear of cutting disks, *Trenie Iznos*, 1993, vol. 14, no. 6, pp. 1115–1117.
20. Aleksandrov, V.A., Zhukovsky, A.N., and Mechnik, V.A., Temperature field and wear of inhomogeneous diamond wheel at convective heat exchange, *Trenie Iznos*, 1994, vol. 15, no. 1, pp. 27–35.
21. Aleksandrov, V.A., Zhukovskij, A.N., and Mechnik, V.A., Temperature field and wear of heterogeneous diamond wheel under conditions of convectional heat transfer. Part 2, *Trenie Iznos*, 1994, vol. 15, no. 2, pp. 196–201.
22. Borowiecka-Jamrozek, J., Microstructure and mechanical properties a new iron-base material used for the fabrication of sintered diamond tools, *Adv. Mater. Res.*, 2014, vol. 1052, pp. 520–523.
23. Borowiecka-Jamrozek, J. and Lachowski, J., Properties of sinters produced from commercially available powder mixtures, *Arch. Foundry Eng.*, 2016, vol. 16, no. 4, pp. 37–40.
24. Konstany, J. and Romanski, A., New nanocrystalline matrix materials for sintered diamond tools, *Mater. Sci. Appl.*, 2012, vol. 3, pp. 779–783.
25. Mechnik, V.A., Bondarenko, N.A., Dub, S.N., Kolodnitskyi, V.M., Nesterenko, Yu.V., Kuzin, N.O., Zakiev, I.M., and Gevorkyan, E.S., A study of microstructure of Fe–Cu–Ni–Sn and Fe–Cu–Ni–Sn–VN metal matrix for diamond containing composites, *Mater. Charact.*, 2018, vol. 146, pp. 209–216.
26. Mechnik, V.A., Bondarenko, N.A., Kolodnitskyi, V.M., Zakiev, V.I., Zakiev, I.M., Ignatovich, S.R., Dub, S.N., and Kuzin, N.O., Effect of vacuum hot pressing temperature on the mechanical and tribological properties of the Fe–Cu–Ni–Sn–VN composites, *Powder Metall. Met. Ceram.*, 2020, vol. 58, nos. 11–12, pp. 679–691.
27. Bondarenko, M.O., Mechnik, V.A., and Suprun, M.V., Shrinkage and shrinkage rate behavior in  $C_{\text{diamond}}$ –Fe–Cu–Ni–Sn–CrB<sub>2</sub> system during hot pressing of pressureless-sintered compacts, *J. Superhard Mater.*, 2009, vol. 31, no. 4, pp. 232–240.
28. Franca, L.F.P., Mostofi, M., and Richard, T., Interface laws for impregnated diamond tools for a given state of wear, *Int. J. Rock Mech. Mining Sci.*, 2015, vol. 73, pp. 184–193.
29. Jialiang, W., Shaohe, Z., and Fenfei, P., Influence mechanism of hard brittle grits on the drilling performance of diamond bit, *J. Annales de Chimie-Science des Materiaux*, 2018, vol. 42, no. 2, pp. 209–220.
30. Bondarenko, N.A., Zhukovsky, A.N., and Mechnik, V.A., Analysis of the basic theories of sintering of materials. 1. Sintering under isothermal and nonisothermal conditions (a review), *Sverkhtverd. Mater.*, 2006, vol. 28, no. 6, pp. 3–17.
31. Kolodnits'kyi, V.M. and Bagirov, O.E., On the structure formation of diamond containing composites used in drilling and stone working tools (A review), *J. Superhard Mater.*, 2017, vol. 39, no. 1, pp. 1–17.
32. Mechnyk, V.A., Regularities of structure formation in diamond–Fe–Cu–Ni–Sn–CrB<sub>2</sub> systems, *Mater. Sci.*, 2013, vol. 49, no. 1, pp. 93–101.
33. Mechnik, V.A., Effect of hot recompaction parameters on the structure and properties of diamond–(Fe–Cu–Ni–Sn–CrB<sub>2</sub>) composites, *Powder Metall. Met. Ceram.*, 2014, vol. 52, nos. 11–12, pp. 709–721.
34. Mechnik, V.A., Bondarenko, N.A., Kolodnitskyi, V.M., Zakiev, V.I., Zakiev, I.M., Ignatovich, S.R., and Yutskevych, S.S., Mechanical and tribological properties of Fe–Cu–Ni–Sn materials with different amounts of CrB<sub>2</sub> used as matrices for diamond-containing composites, *J. Superhard Mater.*, 2020, vol. 42, no. 4, pp. 251–263.

35. Mechnik, V.A., Bondarenko, N.A., Kolodnitskyi, V.M., Zakiev, V.I., Zakiev, I.M., Gevorkyan, E.S., Chishkala, V.A., and Kuzin, N.O., Effect of CrB<sub>2</sub> on the microstructure, properties, and wear resistance of sintered composite and the diamond retention in Fe–Cu–Ni–Sn matrix, *J. Superhard Mater.*, 2021, vol. 43, no. 3, pp. 175–190.
36. Han, P., Xiao, F.R., Zou, W.J., and Liao, B., Effect of different oxides addition on the thermal expansion coefficients and residual stresses of Fe-based diamond composites, *Ceram. Int.*, 2014, vol. 40, no. 3, pp. 5007–5013.
37. Tyrala, D., Romanski, A., and Konstanty, J., The effects of powder composition on microstructure and properties of hot-pressed matrix materials for sintered diamond tools, *J. Mater. Eng. Perform.*, 2020, vol. 29, pp. 1467–1472.
38. Cygan-Baczek, E., Wyzga, P., Cygan, S., Balaand, P., and Romanski, A., Improvement in hardness and wear behaviour of iron-based Mn–Cu–Sn matrix for sintered diamond tools by dispersion strengthening, *Materials*, 2021, vol. 14., p. 1774.
39. Eissa, M., El-Fawahry, K., Ahmed, M.H., and El-Zommor, M., Development of superior high strength low impact transition temperature steels microalloyed with vanadium and nitrogen, *J. Mater. Sci. Technol.*, 1997, no. 5, pp. 3–19.
40. Mechnik, V.A., Bondarenko, N.A., Kolodnitskyi, V.M., Zakiev, V.I., Zakiev, I.M., Storchak, M., Dub, S.N., and Kuzin, N.O., Physico-mechanical and tribological properties of Fe–Cu–Ni–Sn and Fe–Cu–Ni–Sn–VN nanocomposites obtained by powder metallurgy methods, *Tribol. Ind.*, 2019, vol. 41, no. 2, pp. 188–198.
41. Mechnik, V.A., Bondarenko, N.A., Kolodnitskyi, V.M., Zakiev, V.I., Zakiev, I.M., Ignatovich, S.R., Dub, S.N., and Kuzin, N.O., Formation of Fe–Cu–Ni–Sn–VN nanocrystalline matrix by vacuum hot pressing for diamond-containing composite. Mechanical and tribological properties, *J. Superhard Mater.*, 2019, vol. 41, no. 6, pp. 388–401.
42. Han, Y., Zhang, S., Bai, R., Zhou, H., Su, Z., Wu, J., and Wang, J., Effect of nano-vanadium nitride on microstructure and properties of sintered Fe–Cu-based diamond composites, *Int. J. Refract. Met. Hard Mater.*, 2020, vol. 91, p. 105256.
43. Gao, J. and Thompson, R.G., Real time-temperature models for Monte Carlo simulations of normal grain growth, *Acta Mater.*, 1996, vol. 44, no. 11, pp. 4565–4570.
44. Abedinzadeh, R., Safavi, S.M., and Karimzadeh, E., A study of pressureless microwave sintering, microwave-assisted hot press sintering and conventional hot pressing on properties of aluminium/alumina nanocomposite, *J. Mech. Sci. Technol.*, 2016, vol. 30, no. 5, pp. 1967–1972.
45. He, Z. and Ma, J., Grain-growth law during Stage 1 sintering of materials, *J. Phys. D: Appl. Phys.*, 2002, vol. 35, no. 17, pp. 2217–2221.
46. Kodash, V.Y. and Gevorkian, E.S., Pat. 6617271 B1 USA, IC C04B 35/56, 2003.
47. Evans, A.G. and Charles, E.A., Fracture toughness determinations by indentation, *J. Am. Ceram. Soc.*, 1976, vol. 59, nos. 7–8, pp. 371–372.
48. Mechnik, V.A., Bondarenko, N.A., Kolodnitskyi, V.M., Zakiev, V.I., Zakiev, I.M., Kuzin, N.O., and Gevorkyan, E.S., Influence of diamond-matrix transition zone structure on mechanical properties and wear of sintered diamond-containing composites based on Fe–Cu–Ni–Sn matrix with varying CrB<sub>2</sub> content, *Int. J. Refract. Met. Hard Mater.*, 2021, vol. 100, p. 105655.
49. *Selected Powder Diffraction Data for Education and Training (Search Manual and Data Cards)*, USA: International Centre for Diffraction Data, 1988.

*Translated by O. Kadkin*